DISPLACEMENT OF NEWTONIAN LIQUIDS IN CAPILLARY TUBES BY INJECTION OF A PSEUDOPLASTIC METERIAL: FOW PATTERNS MAPPING

Edson José Soares, edson@ct.ufes.br
Group of Flow of Complex Fluids, Department of Mechanical Engineering, Federal University of Espírito Santo, Fernando Ferrari Avenue, 514, Goiabeiras, 29060-900, Vitória, ES, Brazil.
Roney Leon Thompson, roney@cv.uff.br
Group of Flow of Complex Fluids, Applied Mechanic Laboratory, PGMEC, Department of Mechanical Engineering, Federal University Fluminense, Passo da Pátria Street 156, Niterói, 24210-240, RJ, Brazil.
Maxmilian Serguei Mesquita, mesquita@ufes.br
Department of Mechanical Engineering, Federal University y of Espírito Santo, Fernando Ferrari 514, Goiabeiras, 29060-900, Vitória, ES, Brazil.
Márcio Silveira de Carvalho, msc@mec.puc-rio.br
Department of Mechanical Engineering, Pontifical Catholic University of Rio de Janeiro, Marquês de São Vicente street 225, 22453-900, Rio de Janeiro, RJ, Brazil.

Abstract. *An important problem in oil industry nowadays is the process of oil recovery in porous media. In the micro-scale of this media, interfacial forces have a strong influence on the recovery efficiency. The capillary aproach is widly used to represent this micro-scale. An interesting path to investigate is how rheological properties of non-Newtonian fluids can influence on this efficiency. An elliptic mesh generation technique with the Galerkin Finite Element Method is used to compute the liquid-liquid interface of the flow problem of a pseudoplastic material displacing Newtonian viscous liquids in a capillary tube. The constitutive equation is a Generalized Newtonian Fluid (GNF) with the power-law viscosity function. The results were given as a function of a non-Newtonian Capillary number, viscosity ratio and the power-law index. The goal of the present work is to study flow patterns, configuration of the interface between the two phases, and fraction of the mass of Newtonian viscous liquid deposited at the wall, as functions of the dimensionless numbers cited. For shear-thinning material, as the displacing fluid departs from Newtonian behavior the fraction of the mass deposited on the tube wall decreases and the shape of the interface becomes flatter. On the other hand, when shear-thickening material is used as the displacing fluid, the fraction of mass deposited on the tube increases and the shape of the interface becomes sharper.*

Keywords*: liquid-liquid displacement, non-Newtonian liquids, Papanastasiou viscosity function, finite element method, free surface flows.*

1. INTRODUCTION

The displacement of a fluid by gas or liquid injection is a phenomenon that occurs in many industrial processes as well as in some biological flows. The enhanced oil recovery, mucus displacement in pulmonary airways, gas assisted injection molding and coating of catalytic converters are examples of such processes. Generally these two-phase flows take place inside an internal passage characterized by a small length scale. As a consequence, they occur in a laminar regime, sometimes with negligible inertial effects, and the capillary forces play a fundamental role on the cited processes. The configuration of the interface between the gas and liquid, or between the two liquids, is an important result and is strictly related to the effectiveness of the displacing process. An important parameter which can be used to evaluate this effectiveness is the fraction of mass of liquid which is left behind adjacent to the wall. In many practical applications one or both materials exhibits non-Newtonian behavior and therefore the rheological properties of these materials constitute important parameters of the operating window of a typical process since they affect both, the configuration of the interface and the fraction of mass which is left behind. The complete understanding of the displacing mechanism of non-Newtonian liquids, specially concerning the combined effects of interfacial tension and rheological parameters, is in early stages of investigation.

Figure (1) shows a first approximation of the problem described above: liquid 1 displacing the liquid 2 in a capillary tube. The tube is initially occupied by the liquid 1 when the liquid 2 is injected. The phase 1 forms a long bubble that displaces the liquid 2 leaving a fraction of mass behind near to the wall. It is worth noting that this process can be done at constant pressure or at constant flow rate. In the former case, the interfacial front can accelerate while in the latter, the bubble velocity reaches a constant value and the configuration of the interface reaches a fixed shape. When inertia effects can be neglected, however, the interfacial front reaches a constant velocity even for a constant pressure process, as reported in Taylor (1961) and Cox (1962).

For the case when gas is used to displace a Newtonian liquid, this flow has been investigated in a number of theoretical and experimental works after pioneer papers of Fairbrother (1935) and Bretherton (1960). When inertial effects can be neglected, the dimensionless parameter that governs the problem is the capillary number (Ca). This

parameter signifies the ratio of the viscous to interfacial tension forces. For a constant pressure process the capillary number is based on the external pressure which is imposed, since no characteristic velocity exists. For a constant flow rate process or negligible inertia, however, the usual expression for the capillary number is $Ca = \mu U / \sigma$ where, μ is the fluid viscosity, σ is the interfacial tension and U is the displacement velocity.

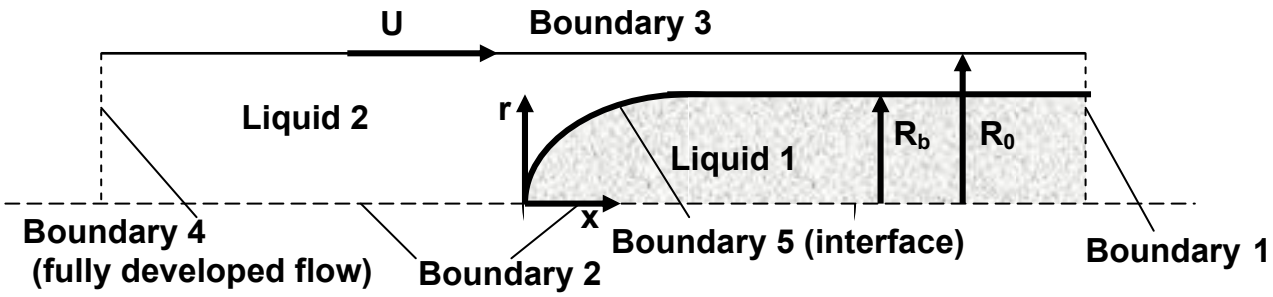

Figure 1 – Schematics of the problem.

Taylor (1961) studied this problem, for a quite large range of capillary number. In his theoretical analysis, he suggested three possible flow regimes of the liquid flow near the interface. The first one, a bypass flow, which would occur at high capillary numbers, the flow would pass completely and no recirculation would appear near the free surface. The other two have recirculation flow patterns. The second one, at a moderate capillary number, the liquid would have a timid recirculation and a stagnation point would arise in the liquid, after the tip of the interface. At low capillary numbers, a third streamline pattern would form when the recirculation of the liquid would have a surface contact with the gas and in this case a stagnation ring would also be formed.

Cox (1962), continuing Taylor's study for a Newtonian viscous fluid, found experimentally that the amount of dimensionless mass *m* deposited on the tube wall asymptotically reaches *0.60* as the capillary number approaches *10*. Here, the dimensionless mass *m* is the ratio between the mass deposited on the wall and the total mass. In a subsequent work, Cox (1964) investigated experimentally the streamline patterns suggested by Taylor and found the two extreme cases suggested, namely, a bypass flow and a fully-recirculation flow for high and low capillary numbers, respectively.

The shear thinning behavior of the displaced liquid in this type of flow was studied Poslinski (1994). They used the finite element method to solve the two-dimensional model of the flow. Kamisli (1999) performed experiments and showed that the thickness of the deposited layer falls with the power-law index. They presented a singular perturbation analysis to model this situation, but their predictions followed the opposite trend of the experimental results. Soares *et al*. (2006) also used the finite element method to analyze shear-thinning effects on gas-liquid displacement and the predictions followed the same trend observed experimentally. Sousa *et al.* (2007), continuing the previews work, investigated the gas-displacement of viscoplastic materials and performed analysis for a wider range of power-law index. They also investigate the streamline patterns near the tip of the interface.

Articles dealing with the analysis of liquid-liquid displacement in capillary tubes are much scarcer. One of these few papers is given by Goldsmith and Mason (1963), who report experimental results on the amount of displaced liquid left on the tube wall as a function of different parameters. In their experiments, the displacing material is a long drop of a viscous liquid. The results showed that the mass fraction rises as the viscosity ratio $N_\mu = \mu_2 / \mu_1$ is decreased, where the index 1 refers to the displacing fluid and μ_2 to the displaced fluid. This trend agrees with the theoretical predictions and experimental data presented Soares *et al*. (2005). They studied the case where a Newtonian viscous liquid was displaced by a long drop of another Newtonian viscous liquid in a capillary tube. The problem was analyzed by numerical simulations and experiments for some governing parameters. The authors investigated the capillary number and viscosity ratio effects on the fractional deposited mass, *m*. They also analyzed the stream line patterns and the shape of the interface tip.

Petitjeans and Maxworthy (1996) analyzed the situation of liquid-liquid displacement with miscible liquids. They studied the effect of the Peclet number, defined as $Pe = V_m D / D_m$, where V_m is the maximum velocity far from the tip of the interface, D the tube diameter, and D_m is the diffusion coefficient. The high Peclet number regime should correspond to the case of immiscible fluids and infinite capillary number.

Free surface problems are inherently nonlinear even for Newtonian fluids under creeping flow conditions because of the nonlinearities introduced by the conditions at the surface boundary. The prediction of the steady flow free surface profile requires therefore a convergent iteration scheme. In the present paper we employ an elliptic grid

generation methodology to study the two-phase flow of a shear-thinning liquid displacing a Newtonian material in a tube via a Galerkin Finite Element Method. The main objective of this work is to investigate numerically how the general results conducted by Goldsmith and Mason (1963), in his classical work concerning liquid-liquid displacement of Newtonian fluids, are sensitive to variation of some non-Newtonian parameters of the displacing liquid. The constitutive equation used to represent the rheological behavior of the displacing liquid was a shear-thinning power-law fluid. The results were presented as flow patterns configuration and the fraction of mass deposited on the tube wall as a function of capillary number, power-law index and the non-Newtonian viscosity ratio.

2. PHISYCAL FORMULATION

2.1. Conservation equations and boundary conditions

The physical model to describe the displacement of a Newtonian liquid of viscosity μ_2 by a long drop of a second non-Newtonian liquid of viscosity η_1 is now presented. The displacing drop (liquid 1) is translating steadily with speed U. To simply the analysis, the governing equations are written with respect to a moving reference frame located at the tip of the interface. In this frame of reference, the flow is steady and the wall is moving with velocity U.

The geometry analyzed is an axisymmetric tube of radius R_0. The liquid is assumed to be incompressible, and the flow is laminar and the inertia is negligible. The velocity and pressure fields are governing by the continuity and momentum equations. In cylindrical coordinates, these governing equations are written as (the subscript $k = 1, 2$ labels the two liquids).

$$0 = \frac{1}{r}\frac{\partial}{\partial r}\left(r v_k\right) + \frac{\partial}{\partial x}\left(u_k\right) \tag{1}$$

$$0 = \left[\frac{1}{r}\frac{\partial}{\partial r}\left(r\tau_{(rx)_k}\right) + \frac{\partial}{\partial x}\left(\tau_{(xx)_k}\right)\right] - \frac{\partial p_k}{\partial x} \tag{2}$$

$$0 = \left[\frac{1}{r}\frac{\partial}{\partial r}\left(r\tau_{(rr)_k}\right) - \frac{\tau_{(\theta\theta)_k}}{r} + \frac{\partial}{\partial x}\left(\tau_{(rx)_k}\right)\right] - \frac{\partial p_k}{\partial r} \tag{3}$$

Where *u* and *v* are respectively the axial and radial components of the velocity field $\boldsymbol{u}$ and the quantities $\boldsymbol{\tau}_{xx}, \boldsymbol{\tau}_{rx}, \boldsymbol{\tau}_{rr}$, and $\tau_{\theta\theta}$ are the components of the stress tensor $\boldsymbol{\tau}$.

In order to facilitate the following description of the boundary conditions, the boundaries are labeled from 1 to 5, as illustrated in Fig. (1).

1) Far enough upstream of the interface, Boundary 4, the flow is taken to be fully developed and the pressure is assumed to be uniform:

$$\mathbf{n}\cdot\nabla\mathbf{u}_2 = 0, \;\; p_2 = p_{in} \tag{4}$$

where $\boldsymbol{n}$ is the unit vector normal to the boundary surface and p_{in} the pressure field.

2) Far enough downstream, Boundary 1, the flow is also assumed to be fully developed, but the pressure is not imposed:

$$\mathbf{n}\cdot\nabla\mathbf{u}_k = 0 \tag{5}$$

3) Along the symmetry axis, Boundary 2, both the shear stress and the radial velocity vanish:

$$\mathbf{t}\cdot\left[\mathbf{n}\cdot\boldsymbol{\tau}_k\right] = \tau_{(rx)_k} = 0\,, \;\; \mathbf{n}\cdot\mathbf{u}_k = 0 \tag{6}$$

where $\boldsymbol{t}$ is a unit vector tangent to the boundary surface.

4) The no-slip and impermeability conditions are imposed along the tube wall, Boundary 3:

$$\mathbf{u} = U\mathbf{e}_x \tag{7}$$

where $\boldsymbol{e}_x$ is the unit vector in the x-direction.

5) At the liquid-liquid interface, Boundary 5, the traction balances the capillary pressure, and there is no mass flow across the interface:

$$\mathbf{n}\left(p_1 - p_2\right) + \mathbf{n}\left(\boldsymbol{\tau}_2 - \boldsymbol{\tau}_1\right) = \frac{\sigma}{R_m}\mathbf{n} \tag{8}$$

$$\left(\mathbf{u}_1 - \mathbf{u}_2\right) = 0 \tag{9}$$

In Eq. (8), $1/R_m$ is the local mean curvature of the interface, defined as

$$\frac{1}{R_m}\mathbf{n} = \frac{1}{\sqrt{x_s^2 + r_s^2}}\frac{\partial \mathbf{t}}{\partial s} - \frac{x_s}{r\sqrt{x_s^2 + r_s^2}}\mathbf{n} \tag{10}$$

where $\boldsymbol{t}$ is the unit tangent vector to the free surface, s is the arc-length curvilinear coordinate along the interface in the r-x plane and $x_s = \partial x/\partial s$ and $r_s = \partial r/\partial s$ are spatial derivatives with respect to s.

2.2. Constitutive equations

In order to close the set of differential equations, the stress tensor was related with the kinematics of the flow by the Generalized Newtonian Fluid model. In this model, the stress tensor is given by

$$\mathbf{T} = -p\mathbf{I} + \eta\left(\dot{\gamma}\right)\dot{\boldsymbol{\gamma}} \tag{11}$$

where $\dot{\boldsymbol{\gamma}} = \nabla\mathbf{u} + \nabla\mathbf{u}^{\mathrm{T}}$ is the rate of strain tensor. The scalar quantity $\eta\left(\dot{\gamma}\right)$ is the viscosity function, and $\dot{\gamma} \equiv \sqrt{\frac{1}{2}tr\left(\dot{\boldsymbol{\gamma}} \cdot \dot{\boldsymbol{\gamma}}\right)}$ is the deformation rate. The viscosity function $\eta\left(\dot{\gamma}\right)$ is the simple power-law function given by Eq. (12).

$$\eta = \kappa\dot{\gamma}^{n-1} \tag{12}$$

where κ is the consistency and n is the behavior index of the fluid.

3. SOLUTION METHOD

3.1 The free boundary problem

Due to the free surface, the flow domain is unknown a priori. In order to solve this free-boundary problem by means of standard techniques for boundary value problems, the set of differential equations and boundary conditions written for the physical domain has to be transformed to an equivalent set, defined in a known reference domain. This subject is better discussed on papers of Kistler and Scriven (1983) and de Santos (1991). This transformation is made by a mapping $\mathbf{x} = \mathbf{x}\left(\boldsymbol{\xi}\right)$ that connects the two domains, as shown in Fig. (2). A functional of weighted smoothness can be used successfully to construct the type of mapping involved here. The inverse of the mapping that minimizes the functional is governed by a pair of elliptic differential equations that are identical to those encountered in diffusional transport with variable diffusion coefficients. The coordinates ξ and η of the reference domain satisfy

$$\nabla \cdot \left(D_\xi \nabla \xi\right) = 0 \text{ and } \nabla \cdot \left(D_\eta \nabla \eta\right) = 0 \tag{13}$$

where D_η and D_ξ are diffusion-like coefficients used to control gradients in coordinate potentials, and thereby the spacing between curves of constant ξ on the one hand and of constant η on the other that make up the sides of the elements that were employed; they were quadrilateral elements. Eq. (13) describes the inverse mapping $\xi\left(x\right)$. To evaluate $x = x\left(\xi\right)$, the diffusion equations that describe the mapping also have to be transformed to the reference configuration.

The gradient of the mapping $x = x(\xi)$ in a two dimensional domain is defined as $\nabla_{\xi} x = \mathbf{J}$, and $\|J\| = \det \mathbf{J}$ is the Jacobian of the transformation. Boundary conditions are needed in order to solve the second-order partial differential equations (13). Spatial derivatives with respect to the coordinates of the physical domain $\boldsymbol{x}$ can be written in terms of the derivatives with respect to the coordinates of the reference domain ξ by using the inverse of the gradient of the mapping

$$\begin{pmatrix} \partial/\partial x \\ \partial/\partial y \end{pmatrix} = J^{-1} \begin{pmatrix} \partial/\partial \xi \\ \partial/\partial \eta \end{pmatrix} \tag{14}$$

Along the solid walls and synthetic inlet and outlet planes, the boundary is located by imposing a relation between coordinates *x* and *y*, and stretching functions are used to distribute the nodal points of the finite element mesh along the boundaries. The free boundary (liquid-liquid interface) is located by imposing the kinematic condition, Eq. (**Erro! Fonte de referência não encontrada.**). The discrete version of the mapping, Eq. (13), is generally referred to as mesh generation equations.

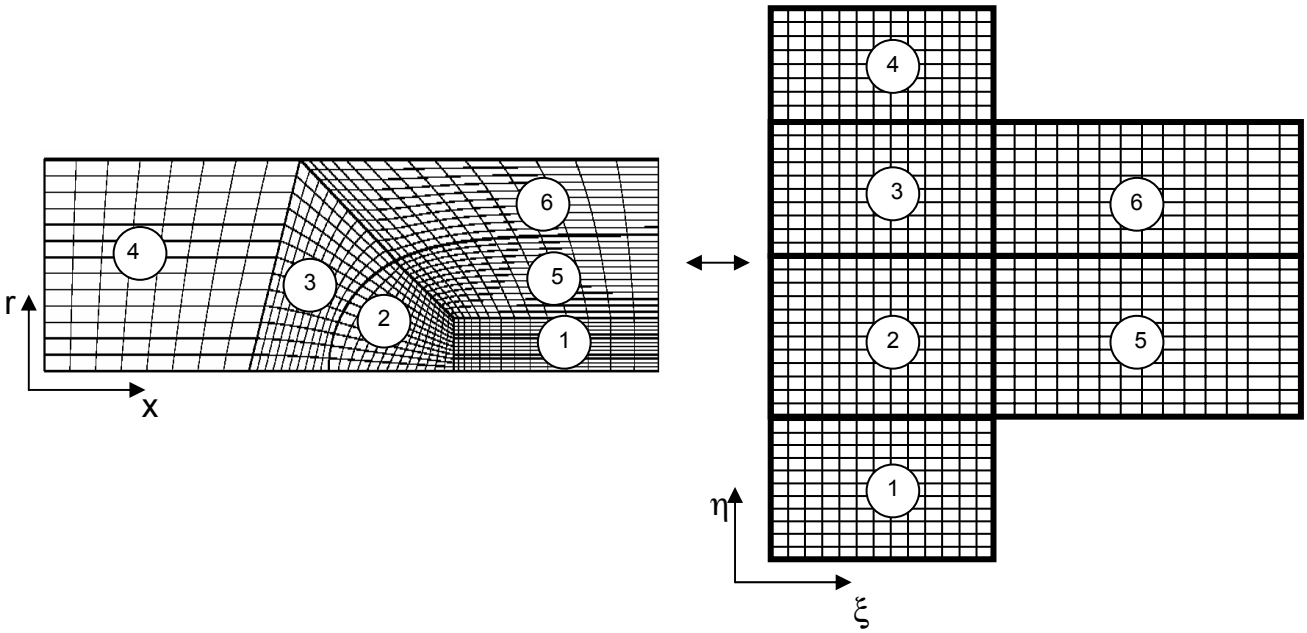

Figure 2 – Mapping between the physical and reference domains.

3.2 Solution of the equation system by Galerkin / Finite Element Methods

The differential equations that govern the problem and the mapping (mesh generation) equations were solved all together by the Galerkin/Finite Element Method. Biquadratic basis functions (ϕ_j) were used to represent the velocity and nodal coordinates, while linear discontinuous functions (χ_j) were employed to expand the pressure field. The velocity, pressure and node position are represented in terms of appropriate basis functions.

$$u = \sum U_j \phi_j ; v = \sum V_j \phi_j ; p = \sum P_j \chi_j ; x = \sum X_j \phi_j ; r = \sum R_j \phi_j \tag{15}$$

The coefficients of the expansions are the unknown of the problem:

$$C = \left[U_j \; V_j \; \mathrm{P_j} \; \mathrm{X_j} \; \mathrm{R_j} \right]^T \tag{16}$$

The corresponding weighted residuals of the Galerkin method related to conservation of momentum, mass and mesh generation are:

$$R^i_{mx} = \int_{\bar{\Omega}} \left[\frac{\partial \phi_i}{\partial x} T_{(xx)_k} + \frac{\partial \phi_i}{\partial r} T_{(xr)_k} \right] r \|J\| d\bar{\Omega} - \int_{\bar{\Gamma}} \mathbf{e}_x \left(\mathbf{n} \cdot \mathbf{T}_k \right) \phi_i r \frac{d\boldsymbol{\Gamma}}{d\bar{\boldsymbol{\Gamma}}} d\bar{\boldsymbol{\Gamma}} \tag{17}$$

$$R_{mr}^{i} = \int_{\bar{\Omega}} \left[\frac{\partial \phi_i}{\partial x} T_{(xr)_k} + \frac{\partial \phi_i}{\partial r} T_{(rr)_k} + \frac{\phi}{r} T_{\theta\theta_k} \right] r \|J\| d\bar{\Omega} - \int_{\bar{\Gamma}} \mathbf{e}_r \left(\mathbf{n} \cdot \mathbf{T}_k \right) \phi_i r \frac{d\boldsymbol{\Gamma}}{d\bar{\boldsymbol{\Gamma}}} d\bar{\boldsymbol{\Gamma}} \tag{18}$$

$$R_{c}^{i} = \int_{\bar{\Omega}} \left[\frac{1}{r} \frac{\partial}{\partial r} \left(r v_k \right) + \frac{\partial u_k}{\partial x} \right] \chi_i r \|J\| d\bar{\Omega} \tag{19}$$

$$R_{\xi}^{i} = -\int_{\bar{\Omega}} D_{\xi} \left(\frac{\partial \phi}{\partial x} \frac{\partial \xi}{\partial x} + \frac{\partial \phi}{\partial r} \frac{\partial \xi}{\partial r} \right) \|J\| d\bar{\Omega} + \int_{\Gamma} D_{\xi} \left(\nabla \xi \cdot \mathbf{n} \right) \phi_i \frac{d\boldsymbol{\Gamma}}{d\bar{\boldsymbol{\Gamma}}} d\bar{\boldsymbol{\Gamma}} \tag{20}$$

$$R_{\eta}^{i} = -\int_{\bar{\Omega}} D_{\eta} \left(\frac{\partial \phi}{\partial x} \frac{\partial \eta}{\partial x} + \frac{\partial \phi}{\partial r} \frac{\partial \eta}{\partial r} \right) \|j\| d\bar{\Omega} + \int_{\Gamma} D_{\eta} \left(\nabla \eta \cdot \mathbf{n} \right) \phi_i \frac{d\boldsymbol{\Gamma}}{d\bar{\boldsymbol{\Gamma}}} d\bar{\boldsymbol{\Gamma}} \tag{21}$$

3.3 Solution of the non-linear system of algebraic equation by Newton's Method

As indicated above, the system of partial differential equations and boundary conditions is reduced to a set of simultaneous algebraic equations for the coefficients of the basis functions of all the fields. This set is non-linear and sparse. It was solved by Newton's method. In order to improve the initial guess there were necessary to solve intermediate problems. The first successful free surface flow was computed using a fixed boundary flow field with slippery surface in place of the free boundary as the initial condition for Newton's method. The linear system of equations at each Newton iteration was solved using a frontal solver. A mesh convergence analysis was done increasing the elements number until the solution changed by less that 1% between successive refinements. The domain was divided into 880 elements that correspond to 3635 nodes and 17180 degrees of freedom. A representative mesh is shown in Fig (3).

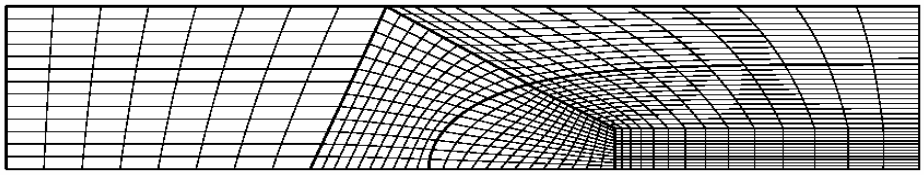

Figure 3 – The finite element mesh, with 880 elements and 17180degrees of freedom.

4. RESULTS

The amount of the liquid 2 that remains on the capillary wall is usually reported in terms of the mass fraction of liquid that is not displaced m , or simply by the liquid film thickness h_∞ left on the wall. The two forms are related by

$$m = \frac{\text{mass left on wall}}{\text{total mass}} = 1 - \frac{\text{displaced mass}}{\text{total mass}}$$
$$= 1 - \left(\frac{D_b}{D_0} \right)^2 = 1 - \left(1 - \frac{2h_\infty}{D_0} \right)^2 \tag{24}$$

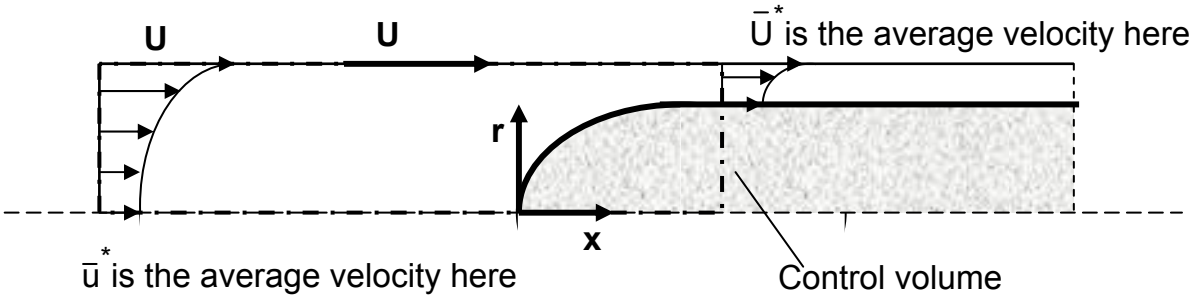

Figure 4 –Velocity profile as measured from a reference frame at the tip of the interface.

The mass fraction of the liquid 2 left on the tube wall can be evaluated using the mass conservation principle for the liquid 2 in a control volume containing the tip of the interface and attached to it. Figure (4) shows this control volume and the sketch of the velocity profiles at inlet and outlet plane as seen from a reference frame attached to tip of the interface. The mass flow rate of the liquid 2 through the control surface upstream of the drop is equal to $\pi R_0^2 \overline{u}^*$ and through the control surface downstream the tip of the interface is $\pi\left(R_0^2 - R_b^2\right)\overline{U}$, $\overline{u}^*$ and $\overline{U}$ being the average velocities of the liquid 2 at the two planes with respect to the moving frame of reference.

The average velocity with respect to the moving frame of reference $\overline{u}^*$ can be evaluated as a function of the average velocity with respect to a fixed frame of reference, $\overline{u}^* = U - \overline{u}$. Applying the mass conservation principle for the displaced liquid on control volume of the Figure 4, $\pi R_0^2 \overline{u}^* = \pi\left(R_0^2 - R_b^2\right)\overline{U}$, the mass fraction m is obtained in terms of the average velocities.

$$m = 1 - \left(\frac{D_b}{D_0}\right)^2 = \frac{U - \overline{u}}{\overline{U}} \tag{25}$$

For a Newtonian liquid displacement of a non inertial incompressible Newtonian liquid, the relevant dimensionless parameters that govern the problem are the Capillary number $\left(Ca\right)$ and Viscosity ratio $\left(N_\mu\right)$. The Capillary number and viscosity ratio are given by

$$Ca \equiv \frac{\mu_2 U}{\sigma} \tag{26}$$

$$N_\mu \equiv \frac{\mu_2}{\mu_1} \tag{27}$$

On the other hand, when the displaced liquid is non –Newtonian, the *Ca* is, again, calculated by Equation (26), but, N_μ must be redefined. It is necessary to choose a characteristic viscosity of the problem. For this purpose the viscosity function is evaluated at the characteristic deformation rate of the flow which is in this problem $\dot{\gamma}_c = U / R$, where *R* is the capillary radius. Hence, the viscosity ratio for the power-law fluid is given by

$$N_\eta = \frac{\mu_2}{\eta_c} = \frac{\mu_2}{K\left(\frac{U}{R}\right)^{n-1}} \tag{28}$$

The rheological dimensionless parameter is the power-law index *n*.

In order to validate the present work, the results are compared with the experiments from Taylor (1961) and Cox (1962) and numerical solution obtained by Souza et al (2006) for gas-liquid displacement. These results are shown in Figure (5). The agreement is quite good over the range of capillarity numbers explored. Figure (6) shown the effect of behavior index, *n*, on the fraction of mass, *m*, deposited on the tube wall as a function of capillary number (in a logarithm scale) for fixed viscosity ratio, $N_\eta = 8$. This figure shows a comparison between three kind of displacing materials, a Newtonian liquid, a shear-thinning liquid with *n = 0.52* and a shear-thickening liquid with *n=1.6*. It can be seen that *m* increases as behavior index is incremented. Figure (7) shows a similar analysis for another fixed value of viscosity ratio, $N_\eta = 4$, and for the same range of power-law index, $0.52 \le n \le 1.6$.

A comparison between Fig. (6) and Fig. (7) indicates that the non-Newtonian effects are more pronounced at small viscosity ratio and at high capillary numbers. Reducing the capillary number the fraction of mass tends to zero and all the curves tends to the Newtonian one. The observations for the viscosity ratio can be explained by the fact that a decreased on the viscosity ratio can be interpreted as an increasing on the characteristic viscosity of the injected material. Hence, the non-Newtonian properties become more pronounced. On the other hand, an increasing of viscosity ratio implies a relative reduction of the characteristic viscosity of the injected material and, therefore, the non-Newtonian properties become less important. The limit case is for $N_\eta \to \infty$ that means the characteristic viscosity approaching zero and hence the non-Newtonian properties plays no influence.

Figure (8) shows flow patterns configuration near the tip of the interface for two values of capillary numbers and power-law index at fixed viscosity ratio, $N_\eta = 4$. The main conclusion here is the fact that the shear thinning behavior of the injected material tends to reduce the recirculation on the displaced liquid.

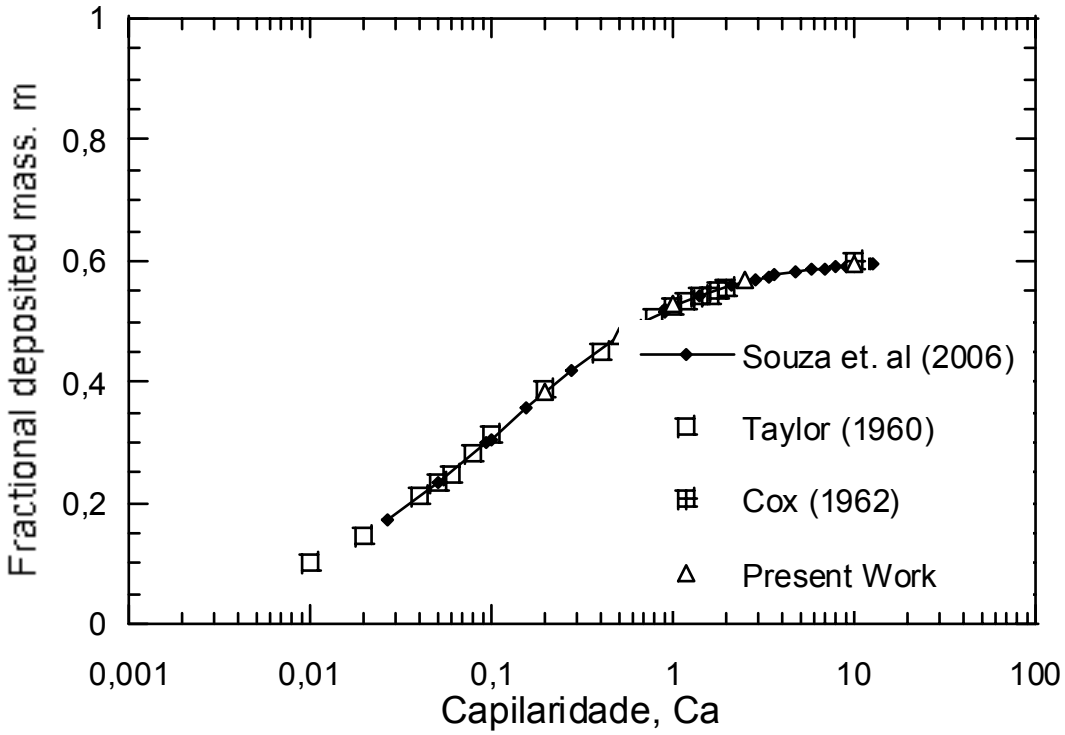

Figure 5 – Fraction of mass deposited on the tube wall as a function of the capillary number. Experimental and Numerical predictions for the case that $N_\mu = 2\times10^4$.

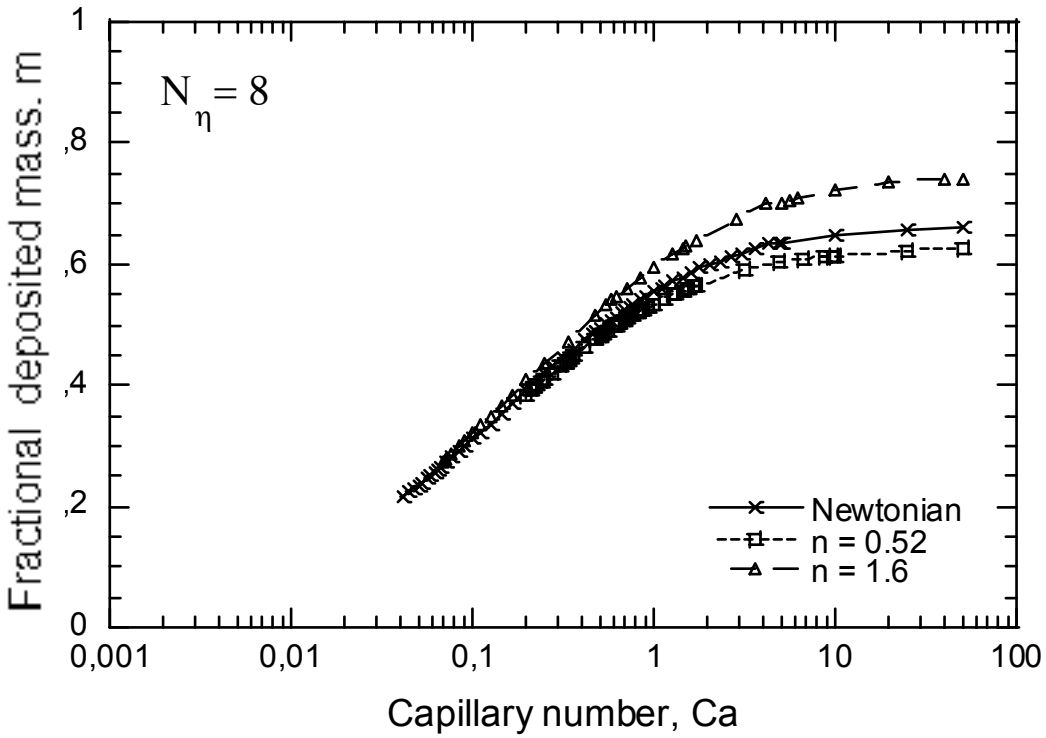

Figure 6 – Fraction of mass deposited on the tube wall as a function of capillary number for fixed viscosity ratio and different values of power-law index.

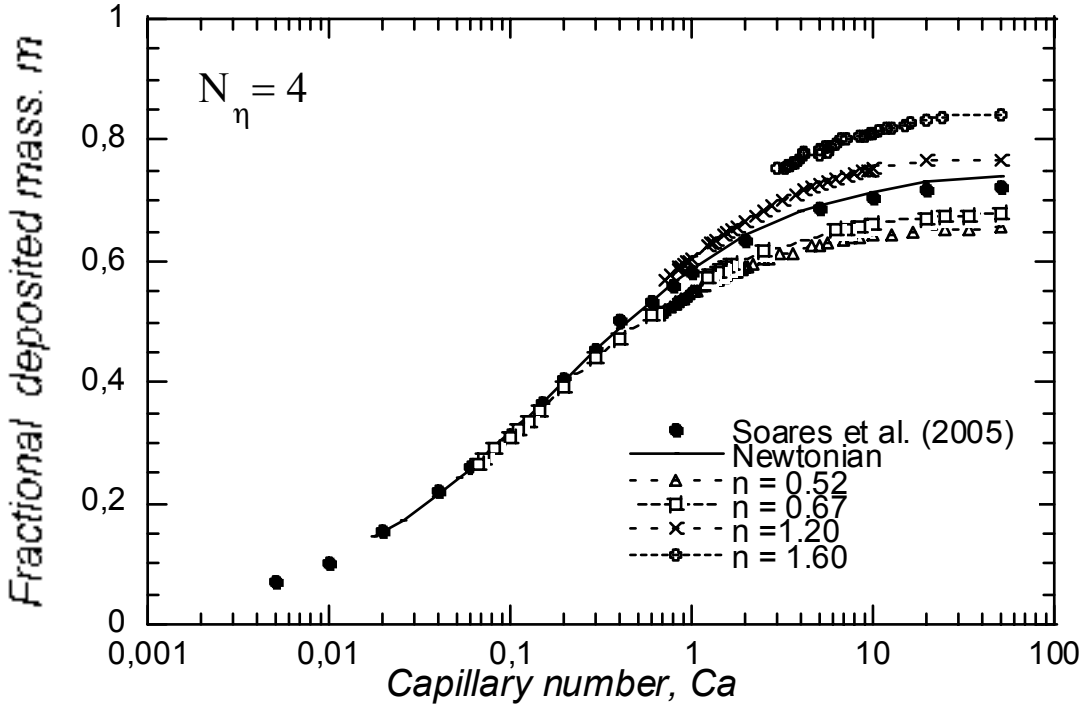

Figure 7 – Fraction of mass deposited on the tube wall as a function of capillary number for fixed viscosity ratio and different values of power-law index.

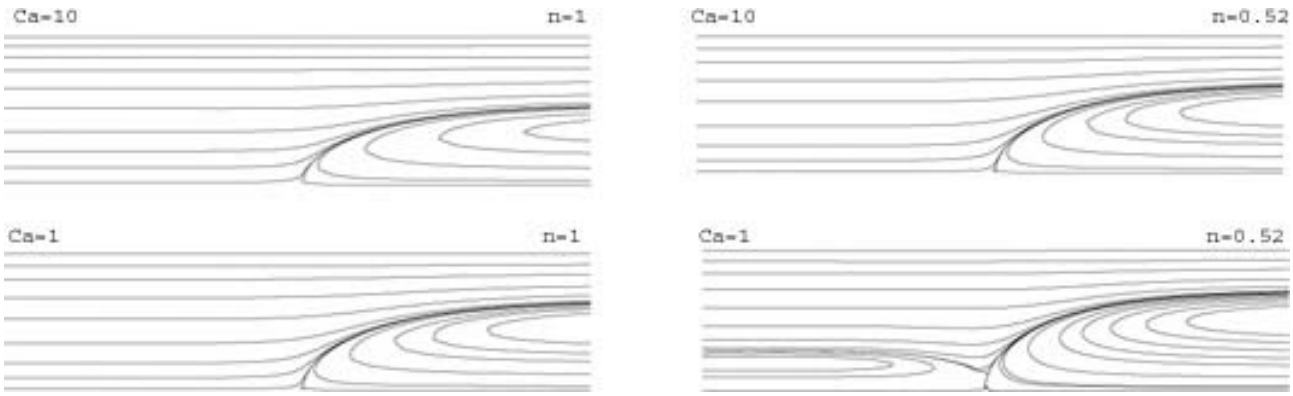

Figure 8 – Stream line patterns near the tip of the interface: comparison between Newtonian and pseudoplastic materials for a fixed viscosity ratio, $N_\eta = 4$.

5. CONCLUSIONS

An axisymmetric model of the flow near the upstream liquid-liquid interface of a long drop penetrating through a liquid in a capillary tube was presented. The presence of the interface makes the problem complex, since the domain in which the differential equations are integrated is unknown a priori. A fully coupled formulation was used and the differential equations were solved via the Galerkin finite element method.

Recent articles are found in the literature which analyze liquid displacement in tubes. However, these are limited to gas-liquid displacement or to liquid-liquid displacement at rather small capillary Numbers and for two Newtonian fluids. Thus, the main contribution of the present work was to investigate the influence of the power-law index, *n*, of the displacing liquid and the non-Newtonian viscosity ratio on the fraction of mass deposited on the tube wall. The

predictions showed an increase of fractional mass, *m*, with increase of power-law index, *n*. In addiction, the results indicated a more pronounced non-Newtonian effect at small non-Newtonian viscosity ratio. Finally, the predictions suggest that decreasing the power-law index of the displacing liquid the recirculation on the displaced one tends to be reduced.

6. ACKNOWLEDGEMENTS

The authors are thankful to CAPES, MCT/CNPq and ANP, for their financial support.

7. REFERENCES

Bretherton, F. P., 1961, "The Motion of Long Bubbles in Tubes," Journal of Fluid Mechanics, Vol. 10, pp. 166–188.

Cox, B. G., 1962, "On Driving a Viscous Fluid Out of a Tube," Journal of Fluid Mechanics, Vol. 14, pp. 81–96.

Cox, B.G., 1964, "An experimental investigation of the streamlines in viscous fluid expelled from a tube", Journal Fluid Mechanics, Vol. 20 pp. 193–200.

Fairbrother, F., and Stubbs, A. E.,1935, "Studies in Electroendosmosis. Part VI. The Bubble-Tube Methods of Measurement," J. Chem. Soc., Vol. 1, pp. 527–529.

Goldsmith, H. L. and Manson, S.G., 1963, "The Flow of suspensionsthrough tubes," J. Colloid Sci., Vol. 18, pp. 237-261.

Kamisli, F., Ryan, M.E., 1999, "Perturbation method in gas-assisted power-law fluid displacement in a circular tube and rectangular channel", Chem. Eng. J. , Vol. 75, pp. 167–176.

Petitjeans, P., and Maxworthy, T., 1996, ''Miscible Displacements in Capillary Tubes,'' J. Fluid Mech., Vol. 326, pp. 37–56.

Poslinski, A.J. Oehler, P.O., Stokes, V.K., 1995, "Isothermal gas-assisted displacement of a viscoplastic liquid in tubes", Poly. Eng. Sci. Vol. 35, pp. 877–892.

Soares, E. J., Carvalho, M. S., Souza Mendes, P. R., 2005, "Immiscible liquid-liquid displacement in capillary tubes," Journal of Fluids Engineering, Vol. 127 (1), pp. 24-31.

Soares, E. J., Carvalho, M. S., Souza Mendes, P. R., 2006, "Gas-displacement of non-Newtonian liquids in capillary tubes," Int. J. Heat and Fluid Flow, Vol. 27 , pp. 95-104.

Taylor, G. I., 1961, "Deposition of a Viscous Fluid on the Wall of a Tube", Journal of Fluid Mechanics, Vol. 10, pp. 161–165.

Souza, D. A., Soares, E. J., Queiroz, R. S. and Thompson, R. L., 2007, "Numerical investigation on gas-displacement of a shear-thinning liquid and a viscoplastic material in capillary tubes", International Journal of non-Newtonian Fluid Mechanics, in press.

8. RESPONSIBILITY NOTICE

The authors are the only responsible for the printed material included in this paper.